ARTICLE

Modeling hypolimnetic dissolved oxygen depletion using monitoring data

Lester L. Yuan and John R. Jones

Abstract: Eutrophication increases hypoxia in lakes and reservoirs, causing deleterious effects on biological communities. Quantitative models would help managers develop effective strategies to address hypoxia issues, but most existing models are limited in their applicability to lakes with temporally resolved dissolved oxygen data. We describe a hierarchical Bayesian model that predicts dissolved oxygen in lakes based on a mechanistic understanding of the factors that influence the development of hypoxia during summer stratification. These factors include the days elapsed since stratification, dissolved organic carbon concentration, lake depth, and chlorophyll concentration. We demonstrate that the model can be fit to two datasets: one in which temporally resolved dissolved oxygen profiles were collected from 20 lakes in a single state and one in which single profiles were collected from 381 lakes across the United States. Analyses of these two datasets yielded similar relationships between volumetric oxygen demand and chlorophyll concentration, suggesting that the model structure appropriately represented the effects of eutrophication on oxygen depletion. Combining both datasets in a single model further improved the precision of predictions.

Résumé : L'eutrophisation rehausse l'hypoxie dans les lacs et réservoirs, entraînant des effets délétères sur les communautés biologiques. Des modèles quantitatifs aideraient les gestionnaires à élaborer des stratégies efficaces visant les enjeux associés à l'hypoxie, mais l'applicabilité de la plupart des modèles existants est limitée aux lacs caractérisés par des données d'oxygène dissous résolues dans le temps. Nous décrivons un modèle bayésien hiérarchique qui prédit l'oxygène dissous dans les lacs sur la base d'une compréhension mécaniste des facteurs qui influencent le développement de l'hypoxie durant la stratification estivale. Ces facteurs comprennent le nombre de jours passés depuis la stratification, la concentration de carbone organique dissous, la profondeur du lac et la concentration de chlorophylle. Nous démontrons que le modèle peut être calé sur deux ensembles de données, soit un ensemble dans lequel des profils d'oxygène dissous résolus dans le temps ont été obtenus de 20 lacs dans un même État et un autre dans lequel un profil unique a été obtenu pour 381 lacs à la grandeur des États-Unis. Des analyses de ces deux ensembles de données produisent des relations semblables entre la demande volumétrique d'oxygène et la concentration de chlorophylle, ce qui indiquerait que la structure du modèle représente adéquatement les effets de l'eutrophisation sur l'appauvrissement en oxygène. La combinaison des deux ensembles de données en un seul modèle améliore la précision des prédictions. [Traduit par la Rédaction]

Introduction

Anthropogenic nutrient loads have increased phytoplankton growth, and the subsequent decomposition of the associated organic material has increased hypolimnetic hypoxia in lakes since the 1850s (Jenny et al. 2016). Cold-water fish require access to cool water refugia, and these areas are rendered uninhabitable by hypoxia (Coutant 1985; Müller and Stadelmann 2004; Plumb and Blanchfield 2009; Jones et al. 2011; Arend et al. 2011). Warm-water fish generally tolerate hypoxia, but hypoxia, coupled with a warm epilimnion, can cause fish species that require cooler temperatures to experience a "thermal-dissolved oxygen squeeze" (after Coutant 1985), requiring them to select between suboptimal temperatures or oxygen (Arend et al. 2011). Anoxic and hypoxic conditions also alter other biological assemblages, including macroinvertebrates (Doke et al. 1995) and zooplankton (Stemberger 1995). Furthermore, anoxia can increase nutrient loads by mobilizing phosphorus from lake sediments (Nürnberg 1984; Pettersson 1998; Søndergaard et al. 2003).

Management of lakes to address hypoxia would benefit from quantifying the effects of different management actions. Specifi-cally, managers should have tools to determine how a reduction in nutrient loads and associated changes in observed phytoplankton abundance would improve dissolved oxygen (DO) concentrations. Relationships between nutrient concentrations and chlorophyll (Chl) are readily available (Jones and Bachmann 1976), but empirical relationships between Chl and DO concentrations are rarely reported (Jones et al. 2011).

Statistical models linking Chl concentrations to deleterious effects in lakes provide useful tools to environmental managers (Yuan and Pollard 2019). In the case of hypoxia though, at least two major challenges must be addressed. First, in most lakes, oxygen depletion progresses steadily after spring stratification, and therefore, a time series of DO measurements in each lake is typically required to fit a statistical model representing oxygen consumption. Because temporally resolved data are required, existing statistical models of oxygen depletion are based on data from a few lakes (Livingstone and Imboden 1996; Rippey and McSorley 2009), which limits model generality. Multiple regression analysis of synoptic data, consisting of single samples collected at sites across a large spatial scale, yield inferences regarding large numbers of

L.L. Yuan. Office of Water, US Environmental Protection Agency, Washington, DC 20460 Mail code 4304T, USA.
J.R. Jones. School of Natural Resources, University of Missouri, Columbia, MO 65211, USA.
Corresponding author: Lester L. Yuan (email: yuan.lester@epa.gov).

Can. J. Fish. Aquat. Sci. **00**: 1–10 (0000) dx.doi.org/10.1139/cjfas-2019-0294

Published at www.nrcresearchpress.com/cjfas on 2 December 2019.

2

Can. J. Fish. Aquat. Sci. Vol. 00, 0000

Fig. 1. Locations of sampled dimictic lakes used in the analysis. Open circles: National Lake Assessment (NLA); filled circles: University of Missouri (UM). Map drawn with R library map (Becker and Wilks 1993).

lakes (Yuan and Pollard 2017); however, these models may not accurately represent DO dynamics.

Second, the process of oxygen depletion is nonlinear, with DO in the hypolimnion approaching zero asymptotically over time (Müller et al. 2012). This nonlinearity complicates the application of conventional regression models that require linear functions. Different approaches address this difficulty, such as limiting the dataset to lakes where DO remains above zero during summer (Molot et al. 1992). However, this restriction constrains the data to oligotrophic to nearly oligotrophic lakes. Others have focused on modeling the rate of oxygen depletion rather than directly modeling DO concentration (Cornett and Rigler 1980), limiting models to temporally resolved data.

Models representing the mechanisms of oxygen depletion provide an alternative to simple statistical models, but require extensive data so are generally applicable only to individual lakes (Chapra and Canale 1991; Stefan et al. 1996; Hamilton and Schladow 1997). A hybrid model, based on a mechanistic understanding of DO depletion, but still simple enough to statistically fit to data collected at broad spatial scales (Borsuk et al. 2001), may provide the best option for modeling hypolimnetic oxygen depletion over eutrophication gradients. Here, we describe such a model and consider whether it can effectively represent changes in hypolimnetic DO and whether it provides useful insights into the relationship between eutrophication and DO. Moreover, we fit the model to two distinct datasets. The first consists of DO measurements over time at a relatively small number of lakes in a single state (Missouri (MO), USA). The second consists of synoptic measurements collected over the conterminous United States. Finally, we consider whether the two disparate datasets can be combined to further improve model precision.

Materials and methods

The MO state data considered in this analysis were collected by the University of Missouri (UM) during summer from 1989 to 2007 as part of a statewide monitoring effort (Fig. 1). Samples were collected near the dam for each reservoir (hereinafter referred to as lakes for simplicity), where vertical profiles for temperature and DO concentration were measured (YSI model 51B or 550A meters). Composite water samples from a depth of ~0.25 m were transferred to high-density linear polyethylene (HDPE) containers, placed in coolers on ice, and transported to the UM Limnology Laboratory. There, a 250 mL aliquot was filtered (Pall A/E) for determination of total Chl via fluorometry following pigment extraction in heated ethanol (Knowlton et al. 1984; Sartory and Grobbelaar 1984). A second aliquot of filtrate was used to measure dissolved organic carbon (DOC) with a Shimadzu TOC-Vcph.

Individual lakes were sampled on three or four occasions during summer.

National Lakes Assessment (NLA) data were collected during summer (May–September) in 2007 and 2012. In 2007, lakes with surface areas greater than 4 ha, and in 2012, lakes greater than 1 ha were selected and sampled from the conterminous United States using a stratified random sampling design (US EPA 2012). The overall sampling design of the NLA was synoptic (Fig. 1), but 10% of sampled lakes were randomly selected and resampled on a different day after the initial visit. Approximately 20% of lakes were sampled in both 2007 and 2012.

During each lake visit, an extensive suite of abiotic and biological variables was measured. Only brief details on sampling protocols relevant to the current analysis are provided here; more extensive descriptions of sampling methodologies are available elsewhere (US EPA 2007, 2011). At each lake, a sampling location was established in open water at the deepest point (up to a maximum depth of 50 m) or at the midpoint of reservoirs, where a water sample was collected using a vertical, depth-integrated methodology that collected water from the photic zone of the lake (to a maximum depth of 2 m). Multiple sample draws were combined in a rinsed, 4 litre (L) cubitainer. When full, the cubitainer was gently inverted to mix the water, and an aliquot was taken as the water chemistry sample. This subsample was placed on ice and shipped overnight to the Willamette Research Station in Corvallis, Oregon, where Chl and DOC concentration was measured. A multiparameter water quality meter was also used to measure profiles of DO concentrations, temperature, and pH at a minimum of 1 m depth intervals.

We restricted our analysis to seasonally stratified lakes because hypoxic conditions occur more consistently during stratified conditions. We identified lakes that were likely to be seasonally stratified by first computing the lake geometry ratio, defined as the surface area of the lake to the 0.25 power divided by the maximum depth. This metric approximates the relative effects of lake fetch and depth on the stability of stratification, and lakes with geometry ratios less than 3 $m^{-0.5}$ have been shown to exhibit seasonal stratification (Gorham and Boyce 1989). We therefore restricted the MO and NLA datasets to lakes with geometry ratios less than this threshold. Temperature profiles collected within these lakes were then screened, and only those that were stratified at the time of sampling were retained. Stratification was defined operationally as lakes with temperature gradients of at least 1 °C·m^{-1} (Wetzel 2001). MO lakes are generally dimictic, and to improve the comparability between NLA and MO datasets, we also identified NLA lakes that were likely dimictic based on latitude and elevation (Fig. 1). This classification approach adjusts the lake latitude by elevation and then identifies lakes with adjusted latitudes that are greater than 40°N as dimictic (Lewis 1983).

Mean hypolimnetic dissolved oxygen (DO$_m$; i.e., depth-averaged DO) values in lakes sampled by MO and by the NLA were computed from temperature and DO profiles with the same series of steps. First, measurements collected at depths ≤ 1 m were excluded to minimize the effects of surface warming. In some profiles, duplicate measurements of DO and (or) temperature were collected at each depth, and in these cases, the average was used in computations. In MO the depth intervals at which temperature and DO measurements were sampled varied among profiles, so measurements were interpolated to a uniform 1 m depth increment with cubic spline interpolation. In cases where profiles were incomplete, measurements were extrapolated to the maximum depth recorded for the lake. For most of these extrapolations, the deepest measured DO was near zero, and the extrapolation merely extended these near-zero measurements to the full depth of the lake. Only profiles with measurements collected from >50% of the maximum depth were used in the final analysis.

The upper boundary of metalimnion was identified as the shallowest depth at which the temperature gradient was >1 °C·m^{-1}.

Fig. 2. Schematic of the model structure.
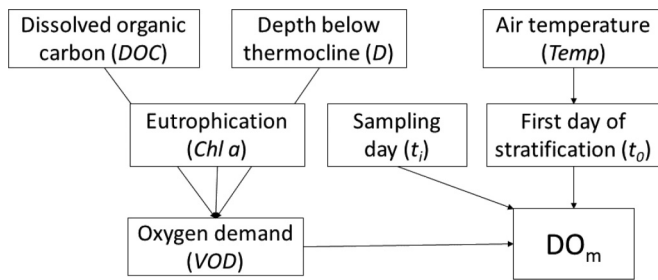
DO$_m$ for each lake profile was computed as the mean of DO measurements estimated at all 1 m increments deeper than the upper boundary of the metalimnion. This estimate of DO$_m$ necessarily includes some measurements in the metalimnion, which may increase our estimates of DO$_m$ relative to studies that can focus only on the hypolimnion. However, many lakes in the MO and NLA datasets were too shallow to maintain a hypolimnion with small vertical temperature gradients (Jones et al. 2011), and therefore, an approach for consistently defining the hypolimnion for all lakes was not available (Quinlan et al. 2005), and we opted to include all depths below the thermocline in our calculation of DO$_m$. The depth of the lake below the thermocline was also computed as the difference between the maximum depth recorded for each lake and the mean depth of the upper boundary of the metalimnion as defined above.

Long-term mean Chl concentration was computed as the mean of the log-transformed Chl measurements. In MO, from four to over 200 measurements were available in each lake with a median value of 32, whereas in NLA, only one to two measurements were available.

Prior to statistical analysis, predictor variables (Chl, DOC, sampling day, and depth below the thermocline) were standardized for both MO and NLA datasets by subtracting their overall mean value (using only NLA data) and dividing by their standard deviation. This standardization had no effect on the final model results, but helped the Bayesian models converge more efficiently (Gelman and Hill 2007).

Statistical model

We modeled the decrease in DO$_m$ as a linear function, an approximation that is appropriate for DO$_m$ concentrations that are greater than $\sim$2 mg·L^{-1} (Burns 1995). This threshold reflects experimental evidence suggesting that rate of decrease of hypolimnetic DO is constant at relatively high ambient concentrations of DO, but can be affected by DO concentrations near zero (Cornett and Rigler 1984). Below, we first describe the statistical model and its application to the MO and NLA data. We then describe our approach for addressing DO$_m$ measurements <2 mg·L^{-1}.

Missouri data

Observed values of DO$_m$ were modeled with a hierarchical Bayesian approach (Gelman and Hill 2007) (Fig. 2). Because temporal data for DO$_m$ were available in the MO dataset, we modeled the observed linear decrease in DO$_m$ concentrations for each unique lake–year combination (Livingstone and Imboden 1996):

(1) $\quad \mathrm{DO}_{m,i} = \mathrm{DO}_0 + \mathrm{VOD}_{k(i)}[t_i - t_{0,j(i)}] + e_{1,i}$

where DO$_0$ is the value of DO$_m$ at the start of spring stratification, the volumetric oxygen demand (VOD$_{k(i)}$) is defined as the net imbalance in the volumetric oxygen budget, expressed as milligrams per litre per day of DO (Burns 1995) for lake, k, corresponding to sample i. The measurement t_i is the date that sample i is collected, and $t_{0,j(i)}$ is the date of the beginning of stratification for lake–year

j corresponding to sample i. The residual error term e_1 is assumed to be normally distributed with a standard deviation of σ_1. Mean minimum air temperature in MO is 7 °C, and we assumed that deepwater lake temperatures at the time of stratification were closely associated with this minimum air temperature. Therefore, we set DO$_0$ to 11.8 mg·L^{-1}, which corresponds to the saturation concentration of DO at this temperature and at the mean elevation of MO.

The parameter t_0 was estimated for each lake–year when fitting the model. Because the number of available samples for each lake–year varied, we defined a hierarchical structure, such that values estimated for t_0 for each lake–year were related to one another via hyperparameters. That is, we defined a distribution for t_0 from which we drew individual values for each lake–year. In this way, parameter estimates for lake–years with relatively sparse data could borrow strength from the overall trends observed across the entire dataset (Gelman and Hill 2007).

The distribution for t_0 was further specified to accommodate the fact that the first day of stratification has been observed to be a function of mean annual air temperature, as modeled by the following relationship (Demers and Kalff 1993):

(2) $\quad t_{0,j} = b_1 + b_2 \mathrm{Temp}_{k(j)} + e_{2,j}$

where Temp$_{k(j)}$ is the mean annual air temperature at the location for lake k, corresponding to lake–year j, and b_1 and b_2 are coefficients that are fit to the data. The published relationship in Demers and Kalff (1993) provided initial estimates for b_1 and b_2, which we used to specify prior distributions for these two parameters. These prior distributions consisted of normal distributions with mean values equal to the estimates provided by Demers and Kalff (1993). Confidence intervals for the parameter values were not available, so weakly informative standard deviations for these prior distributions were specified that were of the same magnitude as the mean value. The error term e_2 is included in the model because the first day of stratification varies substantially in different years for a given lake due to differences in weather. Data published by Demers and Kalff (1993) suggested that the standard deviation of residual error for this relationship was $\sim$12 days, so we used this value to specify the prior distribution for the standard deviation of e_2. This prior was specified as a weakly informative normal distribution, with a mean value of 12, which was then scaled with the same transformation as was applied to sampling day. The error term e_2 also provides a constraint on possible values of $t_{0,j}$, such that lakes with fewer samples for estimating the first day of stratification could borrow strength from lakes with more data.

The parameter VOD was estimated for each lake when fitting the model. Lake trophic status affects VOD because increased phytoplankton production in the epilimnion increases the quantity of organic material available for decomposition in the hypolimnion and in the lake sediments (Hutchinson 1938). VOD also has been observed to decrease with increasing hypolimnion depth, a phenomenon that is attributed to a weaker overall influence of sediment oxygen demand as the volume of the hypolimnion increases (Cornett and Rigler 1980; Müller et al. 2012). In many lakes, allochthonous sources also provides organic matter that fuels bacterial respiration and depletes oxygen in deep lake waters (Pace et al. 2004; Kritzberg et al. 2004), and DOC provided a means of approximating this allochthonous organic matter (Hanson et al. 2003; Cole et al. 2011). Based on these considerations, we modeled the distribution of possible values of VOD as a linear function of the long-term mean Chl concentration, depth below the thermocline, and DOC in each lake:

(3) $\quad \mathrm{VOD}_k = d_1 + d_2 \log(\mathrm{Chl}_k) + d_3 D_k + d_4 \log(\mathrm{DOC}_k) + e_{3,k}$

4

Can. J. Fish. Aquat. Sci. Vol. 00, 0000

where d_1, d_2, d_3, and d_4 are model coefficients estimated from the data, $\log(\text{Chl}_k)$ is the long-term mean of the log-transformed Chl concentration in lake k, D_k is the depth below the thermocline of lake k, and $\log(\text{DOC}_k)$ is the mean of log-transformed DOC concentrations. The error term e_3 quantifies the degree to which VOD estimated for an individual lake k deviates from the trend observed among all lakes. This term was assumed to be normally distributed with mean of zero and a standard deviation of σ_2. As with the model for t_0, the error term e_3 provides a constraint on possible values of VOD, such that lakes with fewer samples can borrow strength from more data-rich lakes.

Prior distributions were based on literature values where available (specifically, parameters associated with predicting the first day of stratification). Other parameters were generally assigned weakly informative prior distributions; however, initial modeling attempts indicated that the prior distribution of the parameter d_1 needed more specificity to ensure that VOD was estimated as a negative value and the model simulation remained stable. Hence, the prior distribution of d_1 was specified as a normal distribution with a mean value of -2 and a standard deviation of 1. Prior distributions for the other coefficients in eq. 3 were specified as normal distributions, with mean values of zero and standard deviations of 3. Prior distributions for the variances (σ_1 and σ_2) were also weakly informative and specified as half-Cauchy distributions with scales of 3. All of the relationships described above were fit simultaneously with RStan (Stan Development Team 2016), which implements the No-U-Turn variance of the Hamiltonian Monte Carlo simulation. We used R (R Core Team 2017) for all other calculations.

NLA data

In the NLA data, as noted previously, only 10% of lakes were sampled again after the initial visit, resulting in poor temporal resolution of changes in DO_m within individual lake–years. Thus, we did not attempt to estimate relationships for each lake–year. Instead, we specified that the observed NLA data was consistent with the same model we specified for the MO data. That is, we fit the NLA data to the following model equation, which combines eqs. 1 and 3:

$$(4) \quad \text{DO}_{m,i} = \text{DO}_0 + [d_1 + d_2 \log(\text{Chl}_i) + d_3 D_i \\ + d_4 \log(\text{DOC}_i)](t_i - t_0) + e_{3,i}$$

where the parameters DO_0, d_1, d_2, d_3, d_4, and t_0, have the same interpretation as described above. By fitting this model, we assumed that we could estimate the depletion of DO_m by fitting relationships to single samples collected at different lakes. That is, we use a space-for-time substitution to estimate temporal changes from differences in space (Meerhoff et al. 2012).

As with the MO data, the first day of stratification (t_0) was not measured for any of the lakes, so we again modeled the first day of stratification as a function of mean annual temperature using the same linear relationship as described in eq. 2. Also, similar to the model for the MO data, we assumed that DO_0, the initial concentration of DO at the time of stratification, was the saturation concentration at the average minimum air temperature at the lake location. Minimum air temperatures less than 4 °C were set to 4 °C, corresponding to deepwater temperatures when the lake surface begins to freeze (Demers and Kalff 1993). Estimates of initial concentrations of DO ranged from 8.8 to 13.1 mg·L⁻¹ in the NLA lakes.

In contrast with the model fit to the MO data, only a single error term, e_3, quantifies the residual variability about the mean trends estimated by the model and is specified as a normal distribution with a mean of zero and standard deviation of σ_3. Combining the different sources of error into one term was necessitated by the fact that only one observation was available from most of the lakes,

Fig. 3. Examples illustrating data selection for Missouri (MO) data. Open circles: observed data not selected for modeling; filled circles: observed data selected for modeling; solid line: estimated mean relationship; gray shading: 90% credible intervals on estimated mean relationship. Left panel: mean hypolimnetic dissolved oxygen (DO_m) greater than 2 mg·L⁻¹ selected for analysis. Asymptotic relationship with time is evident with lower concentrations. Right panel: increase in DO_m after second sample may indicate the occurrence of a mixing event. Solid lines show model estimated relationship between sampling day and DO_m.
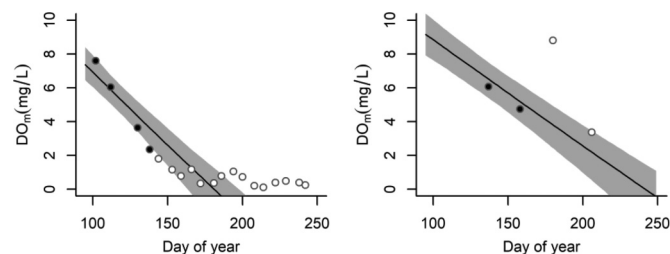
and data were not available to estimate a lake-specific error term. For values of DO_m near zero, the normal residual distribution could potentially yield estimates of DO_m that were less than zero; however, the model was structured to accommodate these negative values (see below).

Prior distributions for the NLA model were identical to those used in the MO model, except for the prior distribution for d_1. In the NLA model, d_1 was also assigned a weakly informative prior normal distribution with a mean value of zero and a standard deviation of 3.

Low DO concentrations

In the MO dataset, we could exclude samples in which DO_m concentration was less than 2 mg·L⁻¹ and still retain enough data in the modeled lakes to estimate a temporal trend in DO_m (left panel, Fig. 3). Because a full temporal history of DO_m was available for each lake–year, we also excluded samples in which DO_m increased from the previous measurement because these increases likely reflected downward transport of DO corresponding to large episodic physical disturbances (right panel, Fig. 3) (Burns 1995). Only lake–years with at least two measurements of DO_m after the exclusions were applied were retained for further analysis.

In the NLA dataset, because only a single DO_m profile was available from most sampled lakes, applying the same exclusion approach would have yielded a biased subsample of the data. That is, the exclusion would have removed more lakes with high VOD than low VOD simply because DO_m in such lakes would be more likely to be measured as <2 mg·L⁻¹. Excluding samples in the MO data did not introduce this bias because at least two measurements of DO_m > 2 mg·L⁻¹ were available in most lakes. That is, samples were excluded from the MO dataset, rather than lakes. However, in the NLA, a different approach was required, so we included all samples in the analysis, but specified that samples for which DO_m < 2 mg·L⁻¹ were censored, such that their "true" value of DO_m was unknown but their maximum value was 2 mg·L⁻¹. A noninformative prior distribution was specified for each censored value of DO_m. This censoring approach retained some information inherent in a sample with DO_m < 2 mg·L⁻¹ (i.e., Chl concentration, lake depth, DOC, and sampling day are consistent with very low DO_m) but allowed us to use linear relationships in the model to estimate the rate of DO depletion. More specifically, with the space-for-time substitution, the model fits a linear trend in time to DO_m observed from lakes with similar Chl, DOC, and depth. Measurements of DO_m < 2 mg·L⁻¹ are assumed to be unknown and are each represented in the Bayesian model as a distribution of possible values that are less than 2 mg·L⁻¹. Compared with the individual measurements of DO_m that were greater than

Fig. 4. Observed DO_m versus chlorophyll (Chl), sampling day, dissolved organic carbon (DOC), and depth below the thermocline. Open circles: NLA; filled circles: MO.
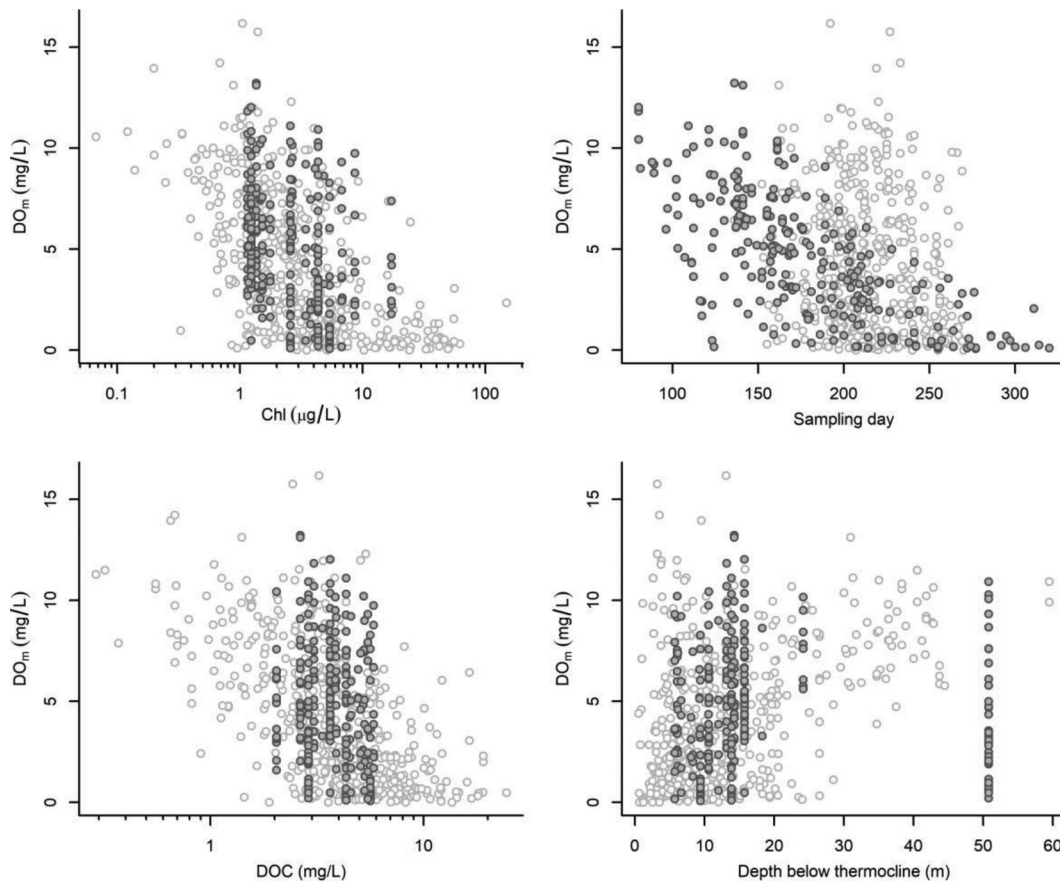
Table 1. Correlation coefficients between different covariates and mean hypolimnetic dissolved oxygen (DO_m) for the Missouri data set (MO) and the National Lakes Assessment dataset (NLA).

	MO	NLA
Chlorophyll	−0.34	−0.58
Sampling day	−0.69	−0.17
DOC	−0.27	−0.61
Depth below thermocline	0.00	0.44

2 mg·L^{-1} and retained in the model, these distributions exerted much less influence on the estimates of the overall relationships because they provide less information. Furthermore, model predictions for these censored values can be less than zero. Such values are not physically possible but are consistent with the linear trends estimated with the rest of the data.

Combined model

In addition to the model for the MO data and the model for the NLA data, we fit a third model that simultaneously fit data observed in both the NLA and MO. Because the basic model equation is identical, the structure of this combined model was identical to the models for each dataset described above. In the case of the combined model, though, both datasets informed estimates of the model coefficients relating mean annual temperature to the first day of stratification and relating VOD to Chl, depth below the

thermocline, and DOC. Prior distributions specified for the combined model were identical to those specified for the NLA model.

Results

After data selection was applied, the final MO dataset consisted of 198 measurements of DO_m collected from 20 lakes and 62 unique lake–year combinations. From two to four measurements were available for most lake–years, but in four lake–years, additional measurements were available ($N = 5$ to 14 samples). In the NLA, a total of 477 measurements from dimictic lakes were analyzed, collected in 381 distinct lakes in either 2007 or 2012. 68 lakes were visited in both of the years, while in 28 unique lake–year combinations, measurements on two different lake visits were collected.

The range of values spanned by each of the covariates differed between the two datasets. MO measurements were collected over a broader range of days compared with the NLA, whereas lakes sampled by the NLA covered a broader Chl range (Fig. 4). Variations in DOC concentrations and depths below the thermocline were also narrower in MO compared with the NLA data. These differences in the range of observations were reflected in the strength of correlation between each covariate and DO_m. In MO, sampling day was most strongly correlated with DO_m, whereas in the NLA it was the weakest correlate of the variables considered (Table 1). Instead, in the NLA, Chl, DOC, and the depth below the thermocline were all correlated more strongly with DO_m.

The modelled fits between DO_m and sampling day (Fig. 3; also refer to online Supplemental Information[1]) reflected the con-

---

Pagination not final (cite DOI) / Pagination provisoire (citer le DOI)

6

Can. J. Fish. Aquat. Sci. Vol. 00, 0000

Fig. 5. Relationship between mean annual temperature and first day of stratification. Filled circles and dashed line: data and model fit replotted from Demers and Kalff (1993); open circles: predicted first day of stratification in NLA lakes from combined NLA–MO model; filled inverted triangles: predicted first day of stratification from MO lakes from combined NLA–MO model; solid line: predicted relationship between mean annual temperature and first day of stratification from combined model; gray shading: 90% credible interval on mean relationship.
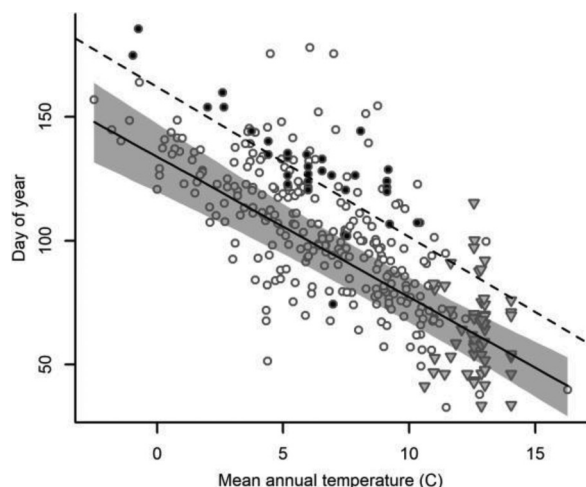
straining influence of hyperdistributions specified in the model. Specifically, in lake–years when observed DO_m decreased rapidly with sampling day, the estimate was slightly less steep than suggested by simple regression. Attenuation of the steepest and shallowest slopes toward the overall mean among all lake–years improves the overall model accuracy (Gelman and Hill 2007) and reflects the fact that extreme observations in a distribution often are random events whose mean expectations are closer to the overall mean than raw data would suggest (Efron and Morris 1977).

For dimictic lakes, Demers and Kalff (1993) reported values of 164 and −6.03 for the coefficients b_1 and b_2 (dashed line in Fig. 5). Model estimates (90% credible intervals in parentheses) based only on the MO data were 107 (73, 158) and −3.00 (−7.06, −0.26). Model estimates based only on the NLA data were 126 (106, 143) and −7.77 (−9.49, −6.09). Estimates using both MO and NLA data were most precise and most similar to the values of Demers and Kalff (1993), with b_1 = 134 (120, 147) and b_2 = −5.68 (−6.83, −4.54). Using the combined model, the estimated first day of stratification ranged from day 50 to day 180 in the NLA lakes (Fig. 5). The combined model estimates of the average first day of stratification, however, were earlier by ~1 month than those reported by Demers and Kalff (1993). The first day of stratification for MO lakes was also earlier than most of the dimictic lakes considered in the national model (Fig. 6), which is consistent with the geographic location of MO at the southern margin of the distribution of dimictic lakes (see Fig. 1).

Models for each dataset accurately predicted observed DO_m (Fig. 7) with a root mean square (RMS) error for the MO data of 1.0 mg·L⁻¹ and an RMS error of 1.5 mg·L⁻¹ for the NLA samples with DO_m > 2 mg·L⁻¹. RMS errors based on the combined model were virtually unchanged from the errors computed for models based on individual datasets. Model coefficients estimated for the two datasets were strikingly consistent (Fig. 8). Because of the standardization applied to the predictor variables, the coefficient d_1 quantifies VOD in a lake with conditions similar to an average NLA lake, with Chl = 2.9 μg·L⁻¹, depth below the thermocline = 13 m, and DOC = 3.7 mg·L⁻¹. Mean values for this parameter for the MO and NLA datasets were −0.073 and −0.059, respectively, but 90% credible intervals for these two estimates overlapped with

Fig. 6. Posterior distribution of mean first day of stratification (t_0) estimated for different lake–years in MO (left panel) and for the NLA (right panel).
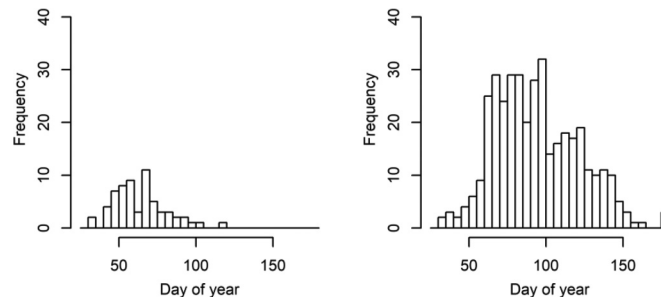

Fig. 7. Predicted DO_m versus observed DO_m for MO (left panel) and NLA (right panel). Solid line shows the 1:1 relationship. Only observed values of DO_m > 2 mg·L⁻¹ are shown.
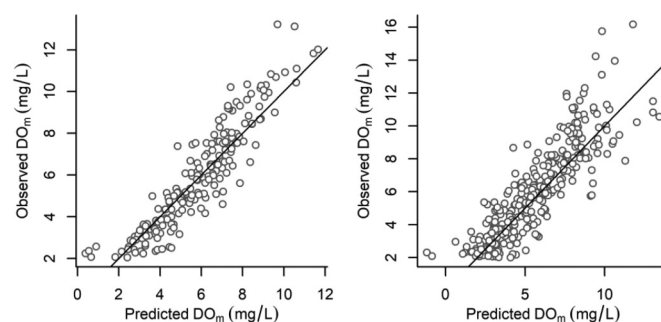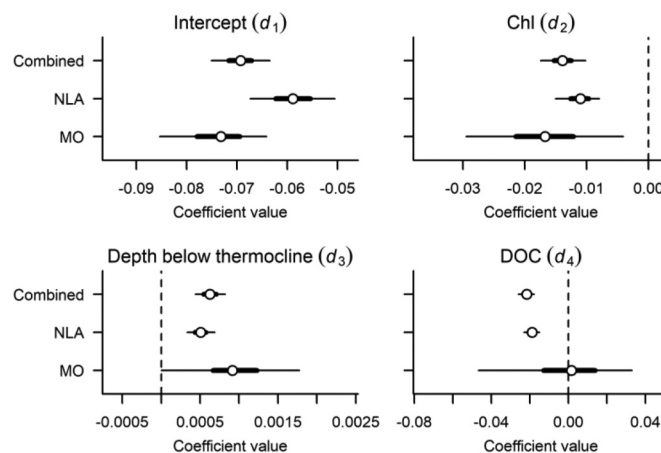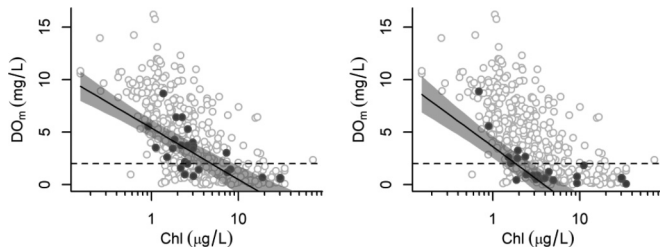

Fig. 8. Model coefficients estimated for models for MO and NLA data and for combined data. Thick line segment: 50% credible intervals; thin line segment: 90% credible intervals. Vertical dashed line shows coefficient value of zero.

one another. For the coefficient d_2, which quantifies the rate of change of VOD with increases in log(Chl), the mean value estimated using only MO data was −0.017, while the mean value estimated using only the NLA data was −0.011. Credible intervals for this parameter also overlapped one another. Finally, estimates of d_3 and d_4, which quantify the relationship between VOD and depth below the thermocline and DOC, were uncertain in MO. The more precise values of these parameters estimated for the NLA data, however, were well within the range of estimates for MO. Here, the limited range of DOC values and depths below thermocline sampled in MO likely limited the precision with which these parameters could be estimated.

Fig. 9. Predicted relationship between Chl and DO_m for different lengths of time between the onset of stratification and the collection of the measurement. Left panel: 120 days; right panel: 150 days. Open circles: all NLA data; filled circles: 20 samples selected with the indicated time lag. Samples were also selected with similar DOC = 3 mg·L^{-1} and depth below thermocline = 10 m to control for the effects of these other covariates. Solid line: predicted mean relationship; gray shading: 90% credible intervals about the mean relationship; dashed horizontal line: $DO_m = 2$ mg·L^{-1}.

Fig. 10. Predicted relationship between Chl and DO_m for different concentrations of DOC. Left panel: DOC = 1 mg·L^{-1}; right panel: DOC = 7 mg·L^{-1}. Symbols as in Fig. 9. Days between stratification and sampling were fixed at 100 days, and depth below thermocline was fixed at 10 m in highlighted samples.


Coefficients for the model based on the combined NLA and MO datasets reflected contributions from each dataset (Fig. 8). For d_3 and d_4, large standard deviations observed in estimates based on only the MO data indicated that little information regarding these coefficients were derived from these data. So, in the combined model, values of d_3 and d_4 were strongly determined by the NLA data. In contrast, estimates of d_1 from MO and NLA data were comparably precise, and the precision of the estimate in the combined model combines information from both datasets to yield an even more precise estimate. The combined estimate of d_2 was slightly more precise than observed for the NLA-only model, reflecting the contribution of a small amount of corroborating data from the MO dataset.

The relationship between Chl and DO_m is of greatest relevance to management decisions, and the current model provides insight into how different factors affect this relationship. Because the length of time between spring stratification and sampling day ($t_i − t_0$) is a multiplicative factor (see eq. 3), increases to $t_i − t_0$ steepen the slope between Chl and DO_m (Fig. 9). That is, increases in the length of time between stratification and the sampling day magnify the effects of higher concentrations of Chl on DO_m. In contrast, changes in the concentration of DOC and the depth below the thermocline are additive factors in eq. 3. Therefore, a change in the value of one of these factors shifts the Chl–DO_m relationship up or down without changing the slope (Fig. 10).

The utility of combining MO and NLA data for informing decision making is evident when one considers the predicted relationship between Chl and DO_m calculated using parameter estimates from the MO data and from the combined MO–NLA dataset (Fig. 11). In the example shown, the relationship is calculated based on illustrative values for other covariates (depth below thermocline = 10 m, DOC = 5 mg·L^{-1}, and time between spring stratification and sampling = 130 days). Because combining the datasets improves the precision of model parameters, the resulting mean relationship is also estimated with increased precision, and a Chl concentration specified to meet a DO_m condition can be identified with greater confidence. In this example, the 50% credible interval for a targeted Chl concentration associated with $DO_m = 0$ extends from 6 to 9 µg·L^{-1} when using the combined model. When just using MO data, the interval expands to 5–10 µg·L^{-1}.

Discussion

We described a model for deepwater hypoxia that accurately predicts DO_m from synoptic surveys of DO profiles at the continental scale and from more temporally intensive measurements from a smaller number of lakes in MO. Recent analyses of continental scale data have revealed insights into broad-scale drivers of lake properties (King et al. 2019; Soranno et al. 2019), and here, we
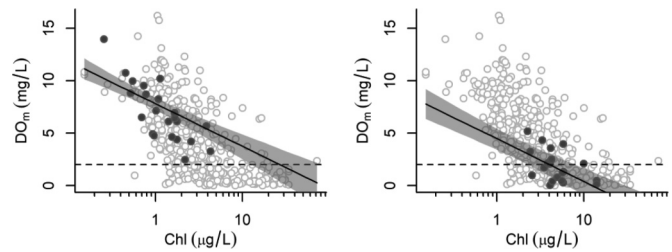
Fig. 11. Relationship between Chl and DO_m in an illustrative lake with depth below thermocline = 10 m, DOC = 5 mg·L^{-1}, and 130 days after spring stratification. Solid line: mean relationship; gray shading: 50% credible intervals about mean relationship from combined MO–NLA model; dashed line: 50% credible intervals about mean relationship from MO-only model; dotted line: $DO_m = 0$ mg·L^{-1}.
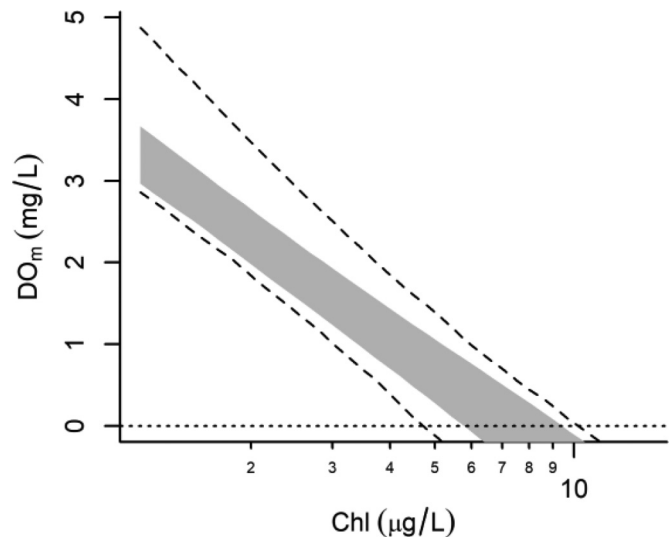
extend these ideas to consider lake hypoxia. The model structure is based on known relationships, in which DO_m decreases over time and the rate of decrease (i.e., the VOD) is associated with lake trophic status and morphology. Because of these mechanistic underpinnings, we believe that this empirical model is broadly applicable to dimictic lakes and useful for guiding management decisions.

The model predicts changes in DO_m among lakes and over time, whereas most other empirical studies of hypolimnetic DO focused analyses on the rate of oxygen depletion (Cornett and Rigler 1980; Müller et al. 2012). Instead of calculating oxygen demand separately, we expressed oxygen demand as a parameter in the overall model for DO_m. The advantages of this approach are threefold. First, DO_m is causally associated with ecological effects in lakes because it defines the extent of viable habitat in deep waters for different organisms. Hence, predictions of DO_m are directly relevant to management decisions. Predictions of oxygen demand require further assumptions and calculations before they achieve this same level of relevance (Nicholls 1997). Second, measurement errors associated with estimating oxygen demand are considered with other sources of error in the model. In studies where oxygen demand is computed in a separate step, this source of error is usually ignored, an omission that can lead to erroneous inferences regarding the uncertainty of model predictions. Third, the model can be

readily applied to a broad variety of datasets, in which DO measurements are not necessarily repeated over time. This last feature broadens the variety of lakes that can be modeled, allowing a deeper examination of differences among lakes that can influence the rate of oxygen dynamics. In this study, we considered the effects of differences in the first day of stratification, Chl, depth, and DOC on observed DO_m.

First day of stratification is critical for predicting DO_m because it fixes the starting point for depletion in waters below the thermocline and therefore determines the timing of DO_m decreases below different concentrations over the remainder of the season (Biddanda et al. 2018). Identifying initial stratification day requires intense field effort, and consequently, measurements of this day are rare. Our model provides an alternate approach for estimating initial stratification day based on "hindcasting" from current conditions. The resulting estimates of stratification day exhibited a decreasing relationship with mean annual temperature as reported previously (Fig. 5), but our estimate of stratification day for a given mean annual temperature was somewhat earlier. This difference may be attributed to a combination of factors. First, data used by Demers and Kalff (1993) were based on profiles collected at biweekly to monthly intervals, and because of this coarse temporal resolution, the reported first day of stratification was probably later than the actual day. Second, the implied definition of stratification used in the current model is a state in which vertical transport of DO is restricted, a definition that differs from a typical approach of examining temperature gradients in vertical profiles. The present definition of stratification focuses on the effects of stratification rather than on a single threshold temperature gradient that may vary in relevance among lakes. Finally, our assumption regarding the initial DO_m concentration affects estimates of t_0, and further work testing this assumption is merited.

Improvements in the estimates of the first day of stratification in the combined model demonstrate the utility of including different data sources in a single model. The temporally intense MO data allowed us to estimate the first day of stratification by fitting a linear trend to repeated measurements of DO_m from individual lakes (Fig. 3). The geographic scope and the associated range of mean annual temperatures in the MO data, however, was limited (Fig. 5), leading to imprecise estimates of the model coefficients. Conversely, in the NLA data, only single samples were available from most lakes, so fitting linear trends necessarily involved the additional error associated with combining data from many different lakes. The broad geographical scope of the NLA data, however, yielded an improved capacity for estimating the effect of mean annual temperature. Combining these two disparate datasets and estimating a relationship that best accounts for observations in both datasets leverages the available data and yields vastly more precise estimates of the first day of stratification.

We observed strong increases in VOD with increases in Chl, consistent with prevailing understanding of the underlying mechanisms of lake hypoxia and previously shown in MO lakes (Jones et al. 2011). The similarity of relationships estimated using the NLA and MO datasets suggests that the model accurately represented underlying processes. Eutrophication is generally thought to increase the supply of organic matter to the hypolimnion, fueling an increase in oxygen demand. However, datasets measuring oxygen demand across a eutrophication gradient are rare. In oligotrophic lakes in Ontario, end-of-summer DO concentrations were inversely proportional to total phosphorus (TP), suggesting increased productivity even across a limited range of TP was associated with increased oxygen demand (Molot et al. 1992). Similarly, oxygen depletion rates over multiple years in Lake Erie increased with TP (El-Shaarawi 1984). Other retrospective studies have identified point sources of phosphorus as the primary factor causing historical increases in hypoxia (Jenny et al. 2016). Our current analysis provides a quantitative relationship between Chl and VOD for lake with Chl ranging from 1 to nearly 100 $\mu g \cdot L^{-1}$, substantially broadening the range of conditions in which the effects of eutrophication on hypoxia can be predicted.

Long-term Chl is an indicator of autochthonous organic matter loading in different lakes, so it is one causal step removed from the factor that causes oxygen demand. Thus, the lack of direct measurements of organic material in the lakes of this study may account for some of residual variance in the relationship estimated between VOD and Chl (Fig. 11). Of special note, high rates of oxygen demand have been documented in lakes with low Chl, reflecting historical loading of organic material (Jenny et al. 2014).

The effect of hypolimnion depth on oxygen demand has been the subject of substantial debate (Livingstone and Imboden 1996). Our finding of a decrease in the magnitude of VOD with increasing depth below the thermocline was similar to findings from ten Wisconsin lakes (Cornett and Rigler 1980). Others observed that oxygen demand normalized by the surface areas of the hypolimnion (AHOD) increased with depth (Hutchinson 1938; Müller et al. 2012). These different relationships between depth and oxygen demand likely stem from the volumetric versus areal normalizations applied previously, and the uncertainty regarding the correct normalization to apply, in turn, reflect incomplete understanding of the mechanisms that drive oxygen depletion (Livingstone and Imboden 1996; Rippey and McSorley 2009). Because we lacked bathymetric data in most lakes, we were unable to estimate AHOD in this study. We suggest, however, that the modelling approach described here provides a way to incorporate data from a broader variety of lakes to investigate this question.

The strong effect of DOC on oxygen demand was surprising, and in general, the influence of allochthonous carbon on lake hypoxia has received little attention. The possible contribution of allochthonous organic material to bacterial respiration in lakes has been documented in a few studies (Kritzberg et al. 2004; Marcé et al. 2008). The restricted variety of lakes in which temporally resolved DO profiles and DOC data were available, however, likely limited the degree to which DOC effects could be examined. Our current model's capacity for considering data collected at a continental scale allowed an estimate of the effect of DOC, and the lack of a strong effect of DOC in the MO dataset contrasts with that observed in NLA. Lakes sampled in a small geographic area are more likely to have similar DOC concentrations, and hence, the range of DOC concentrations is too narrow to estimate a relationship between DOC and DO_m. Only when a broader variety of lakes and DOC concentrations is considered can the effect be quantified, and indeed, at the continental scales of the NLA, the effect of DOC was as strong as Chl in explaining differences in VOD.

Understanding the correct functional form of the relationship between Chl and DO_m helps guide management decisions. Our model clarifies the fact that the effect of time between spring stratification and the sampling time magnifies the effects of differences in Chl. From a management perspective, this finding highlights the importance of gathering information regarding spring stratification and critical time windows for different species before attempting to estimate targets for management. Furthermore, effects on fish arise from the combined influences of increased temperatures and decreased DO_m, and therefore, the model described here would be most informative if combined with a model for water temperature.

Several assumptions that simplified the model may merit further investigation. Other analyses of hypolimnetic DO have examined changes in DO at discrete depths (Molot et al. 1992; Livingstone and Imboden 1996; Rippey and McSorley 2009), whereas we modeled mean DO concentration over the entire hypolimnion. This simplification was necessitated by the available data and the wide variety of lakes. In short, modeling changes at specific depths requires DO profile measurements in time, which are rarely available from routine monitoring. Similarly, model formulations that predict DO in each depth layer as a function of the lake bottom that is

exposed to the layer (Livingstone and Imboden 1996) was not possible. Here again, we believe that neglecting these effects facilitates the development of a broadly applicable model. Other sources and sinks of DO contribute to overall residual error in the model. In the NLA data, for example, we could not account for downward transport of DO through the thermocline. Also, production of DO in the shallower depths may have been possible and contributed to overall DO balance (Gelda and Effler 2002).

Use of Bayesian hierarchical models was critical for estimating these relationships. The models provide a flexible means of specifying a model structure, which differ from model formats available from conventional linear regression. Also, by specifying prior distributions, we could supply the models with existing knowledge regarding the likely first date of stratification. Finally, Bayesian models provide the ability to specify model parameters that were likely similar and likely different across the two datasets. Ultimately, the model structure specified here can continue to incorporate new data and knowledge as it becomes available (Clark 2005). Overall, we believe that the model described provides a robust framework for developing a quantitative and broad understanding of the factors affecting hypoxia in lakes and reservoirs.

Acknowledgements

References

Arend, K.K., Beletsky, D., DePinto, J.V., Ludsin, S.A., Roberts, J.J., Rucinski, D.K., et al. 2011. Seasonal and interannual effects of hypoxia on fish habitat quality in central Lake Erie. Freshw. Biol. **56**(2): 366–383. doi:10.1111/j.1365-2427.2010.02504.x.

Becker, R.A., and Wilks, A.R. 1993. Maps in S. AT & T Bell Laboratories Statistics Research Report [93.2].

Biddanda, B.A., Weinke, A.D., Kendall, S.T., Gereaux, L.C., Holcomb, T.M., Snider, M.J., et al. 2018. Chronicles of hypoxia: Time-series buoy observations reveal annually recurring seasonal basin-wide hypoxia in Muskegon Lake — a Great Lakes estuary. J. Gt. Lakes Res. **44**(2): 219–229. doi:10.1016/j.jglr.2017.12.008.

Borsuk, M.E., Higdon, D., Stow, C.A., and Reckhow, K.H. 2001. A Bayesian hierarchical model to predict benthic oxygen demand from organic matter loading in estuaries and coastal zones. Ecol. Model. **143**(3): 165–181. doi:10.1016/S0304-3800(01)00328-3.

Burns, N.M. 1995. Using hypolimnetic dissolved oxygen depletion rates for monitoring lakes. N.Z. J. Mar. Freshw. Res. **29**(1): 1–11. doi:10.1080/00288330.1995.9516634.

Chapra, S.C., and Canale, R.P. 1991. Long-term phenomenological model of phosphorus and oxygen for stratified lakes. Water Res. **25**(6): 707–715. doi:10.1016/0043-1354(91)90046-S.

Clark, J.S. 2005. Why environmental scientists are becoming Bayesians. Ecol. Lett. **8**(1): 2–14. doi:10.1111/j.1461-0248.2004.00702.x.

Cole, J.J., Carpenter, S.R., Kitchell, J., Pace, M.L., Solomon, C.T., and Weidel, B. 2011. Strong evidence for terrestrial support of zooplankton in small lakes based on stable isotopes of carbon, nitrogen, and hydrogen. Proc. Natl. Acad. Sci. **108**(5): 1975–1980. doi:10.1073/pnas.1012807108. PMID:21245299.

Cornett, R.J., and Rigler, F.H. 1980. The areal hypolimnetic oxygen deficit: An empirical test of the model: areal hypolimnetic oxygen deficit. Limnol. Oceanogr. **25**(4): 672–679. doi:10.4319/lo.1980.25.4.0672.

Cornett, R.J., and Rigler, F.H. 1984. Dependence of hypolimnetic oxygen consumption on ambient oxygen concentration: fact or artifact? Water Resour. Res. **20**(7): 823–830. doi:10.1029/WR020i007p00823.

Coutant, C.C. 1985. Striped bass, temperature, and dissolved oxygen: A speculative hypothesis for environmental risk. Trans. Am. Fish. Soc. **114**(1): 31–61. doi:10.1577/1548-8659(1985)114<31:SBTADO>2.0.CO;2.

Demers, E., and Kalff, J. 1993. A simple model for predicting the date of spring stratification in temperate and subtropical lakes. Limnol. Oceanogr. **38**(5): 1077–1081. doi:10.4319/lo.1993.38.5.1077.

Doke, J.L., Funk, W.H., Juul, S.T.J., and Moore, B.C. 1995. Habitat availability and benthic invertebrate population changes following alum treatment and hypolimnetic oxygenation in Newman Lake, Washington. J. Freshw. Ecol. **10**(2): 87–102. doi:10.1080/02705060.1995.9663423.

Efron, B., and Morris, C. 1977. Stein's paradox in statistics. Sci. Am. **236**: 119–127. doi:10.1038/scientificamerican0577-119.

El-Shaarawi, A.H. 1984. Dissolved oxygen concentrations in Lake Erie (U.S.A.–Canada): 2. A statistical model for dissolved oxygen in the Central Basin of Lake Erie. J. Hydrol. **72**(3–4): 231–243. doi:10.1016/0022-1694(84)90082-9.

Gelda, R.K., and Effler, S.W. 2002. Metabolic rate estimates for a eutrophic lake from diel dissolved oxygen signals. Hydrobiologia, **485**(1–3): 51–66. doi:10.1023/A:1021327610570.

Gelman, A., and Hill, J. 2007. Data analysis using regression and multilevel/hierarchical models. Cambridge University Press, New York.

Gorham, E., and Boyce, F.M. 1989. Influence of lake surface area and depth upon thermal stratification and the depth of the summer thermocline. J. Gt. Lakes Res. **15**(2): 233–245. doi:10.1016/S0380-1330(89)71479-9.

Hamilton, D.P., and Schladow, S.G. 1997. Prediction of water quality in lakes and reservoirs. Part I — Model description. Ecol. Model. **96**(1–3): 91–110. doi:10.1016/S0304-3800(96)00062-2.

Hanson, P.C., Bade, D.L., Carpenter, S.R., and Kratz, T.K. 2003. Lake metabolism: relationships with dissolved organic carbon and phosphorus. Limnol. Oceanogr. **48**(3): 1112–1119. doi:10.4319/lo.2003.48.3.1112.

Hutchinson, G.E. 1938. On the relation between the oxygen deficit and the productivity and typology of lakes. Int. Rev. Gesamten Hydrobiol. Hydrogr. **36**(2): 336–355. doi:10.1002/iroh.19380360205.

Jenny, J.-P., Arnaud, F., Alric, B., Dorioz, J.-M., Sabatier, P., Meybeck, M., and Perga, M.-E. 2014. Inherited hypoxia: a new challenge for reoligotrophicated lakes under global warming. Global Biochem. Cycles, **28**(12): 1413–1423. doi:10.1002/2014GB004932.

Jenny, J.-P., Normandeau, A., Francus, P., Taranu, Z.E., Gregory-Eaves, I., Lapointe, F., et al. 2016. Urban point sources of nutrients were the leading cause for the historical spread of hypoxia across European lakes. Proc. Natl. Acad. Sci. **113**(45): 12655–12660. doi:10.1073/pnas.1605480113. PMID:27791076.

Jones, J.R., and Bachmann, R.W. 1976. Prediction of phosphorus and chlorophyll levels in lakes. J. Water Pollut. Control Fed. **48**(9): 2176–2182.

Jones, J.R., Knowlton, M.F., Obrecht, D.V., and Graham, J.L. 2011. Temperature and oxygen in Missouri reservoirs. Lake Reserv. Manage. **27**(2): 173–182. doi:10.1080/07438141.2011.583713.

King, K., Cheruvelil, K.S., and Pollard, A. 2019. Drivers and spatial structure of abiotic and biotic properties of lakes, wetlands, and streams at the national scale. Ecol. Appl. **29**(7): e01957. doi:10.1002/eap.1957. PMID:31240779.

Knowlton, M.F., Hoyer, M.V., and Jones, J.R. 1984. Sources of variability in phosphorus and chlorophyll and their effects on use of lake survey data. J. Am. Water Resour. Assoc. **20**(3): 397–408. doi:10.1111/j.1752-1688.1984.tb04722.x.

Kritzberg, E.S., Cole, J.J., Pace, M.L., Granéli, W., and Bade, D.L. 2004. Autochthonous versus allochthonous carbon sources of bacteria: results from whole-lake ^{13}C addition experiments. Limnol. Oceanogr. **49**(2): 588–596. doi:10.4319/lo.2004.49.2.0588.

Lewis, W.M., Jr. 1983. A revised classification of lakes based on mixing. Can. J. Fish. Aquat. Sci. **40**(10): 1779–1787. doi:10.1139/f83-207.

Livingstone, D.M., and Imboden, D.M. 1996. The prediction of hypolimnetic oxygen profiles: a plea for a deductive approach. Can. J. Fish. Aquat. Sci. **53**(4): 924–932. doi:10.1139/f95-230.

Marcé, R., Moreno-Ostos, E., López, P., and Armengol, J. 2008. The role of allochthonous inputs of dissolved organic carbon on the hypolimnetic oxygen content of reservoirs. Ecosystems, **11**(7): 1035–1053. doi:10.1007/s10021-008-9177-5.

Meerhoff, M., Teixeira-de Mello, F., Kruk, C., Alonso, C., González-Bergonzoni, I., Pacheco, J.P., Lacerot, G., Arim, M., Beklioğlu, M., Brucet, S., Goyenola, G., Iglesias, C., Mazzeo, N., Kosten, S., and Jeppesen, E. 2012. 4 - Environmental warming in shallow lakes: a review of potential changes in community structure as evidenced from space-for-time substitution approaches. *In* Advances in Ecological Research, Vol. 46. *Edited by* U. Jacob and G. Woodward. Academic Press. pp. 259–349. doi:10.1016/B978-0-12-396992-7.00004-6.

Molot, L.A., Dillon, P.J., Clark, B.J., and Neary, B.P. 1992. Predicting end-of-summer oxygen profiles in stratified lakes. Can. J. Fish. Aquat. Sci. **49**(11): 2363–2372. doi:10.1139/f92-260.

Müller, B., Bryant, L.D., Matzinger, A., and Wüest, A. 2012. Hypolimnetic oxygen depletion in eutrophic lakes. Environ. Sci. Technol. **46**(18): 9964–9971. doi:10.1021/es301422r. PMID:22871037.

Müller, R., and Stadelmann, P. 2004. Fish habitat requirements as the basis for rehabilitation of eutrophic lakes by oxygenation. Fish. Manage. Ecol. **11**(3–4): 251–260. doi:10.1111/j.1365-2400.2004.00393.x.

Nicholls, K.H. 1997. A limnological basis for a Lake Simcoe phosphorus loading objective. Lake Res. Manage. **13**(3): 189–198. doi:10.1080/07438149709354310.

Nürnberg, G.K. 1984. The prediction of internal phosphorus load in lakes with anoxic hypolimnia1. Limnol. Oceanogr. **29**: 111–124. doi:10.4319/lo.1984.29.1.0111.

Pace, M.L., Cole, J.J., Carpenter, S.R., Kitchell, J.F., Hodgson, J.R., Van de Bogert, M.C., et al. 2004. Whole-lake carbon-13 additions reveal terrestrial support of aquatic food webs. Nature, **427**(6971): 240–243. doi:10.1038/nature02227. PMID:14724637.

Pettersson, K. 1998. Mechanisms for internal loading of phosphorus in lakes. Hydrobiologia, **373**: 21–25. doi:10.1023/A:1017011420035.

Plumb, J.M., and Blanchfield, P.J. 2009. Performance of temperature and dissolved oxygen criteria to predict habitat use by lake trout (*Salvelinus namaycush*). Can. J. Fish. Aquat. Sci. **66**(11): 2011–2023. doi:10.1139/F09-129.

Quinlan, R., Paterson, A.M., Smol, J.P., Douglas, M.S.V., and Clark, B.J. 2005. Comparing different methods of calculating volume-weighted hypolimnetic

Pagination not final (cite DOI) / Pagination provisoire (citer le DOI)

10   Can. J. Fish. Aquat. Sci. Vol. 00, 0000

oxygen (VWHO) in lakes. Aquat. Sci. **67**(1): 97–103. doi:10.1007/s00027-004-0717-6.

R Core Team. 2017. R: a language and environment for statistical computing [online]. R Foundation for Statistical Computing, Vienna, Austria. Available from https://www.R-project.org/.

Rippey, B., and McSorley, C. 2009. Oxygen depletion in lake hypolimnia. Limnol Oceanogr. **54**(3): 905–916. doi:10.4319/lo.2009.54.3.0905.

Sartory, D.P., and Grobbelaar, J.U. 1984. Extraction of chlorophyll *a* from freshwater phytoplankton for spectrophotometric analysis. Hydrobiologia, **114**(3): 177–187. doi:10.1007/BF00031869.

Søndergaard, M., Jensen, J.P., and Jeppesen, E. 2003. Role of sediment and internal loading of phosphorus in shallow lakes. Hydrobiologia, **506–509**(1–3): 135–145. doi:10.1023/B:HYDR.0000008611.12704.dd.

Soranno, P.A., Wagner, T., Collins, S.M., Lapierre, J.-F., Lottig, N.R., and Oliver, S.K. 2019. Spatial and temporal variation of ecosystem properties at macroscales. Ecol. Lett. **22**(10): 1587–1598. doi:10.1111/ele.13346. PMID:31347258.

Stan Development Team. 2016. Stan modeling language users guide and reference manual. Version 2.14.0 [online]. Available from http://mc-stan.org.

Stefan, H.G., Hondzo, M., Fang, X., Eaton, J.G., and McCormick, J.H. 1996. Simulated long-term temperature and dissolved oxygen characteristics of lakes in the north-central United States and associated fish habitat limits. Limnol. Oceanogr. **41**(5): 1124–1135. doi:10.4319/lo.1996.41.5.1124.

Stemberger, R.S. 1995. The influence of mixing on rotifer assemblages of Michigan lakes. Hydrobiologia, **297**(2): 149–161. doi:10.1007/BF00017481.

US EPA. 2007. Survey of the Nation's lakes: field operations manual. Office of Water, US Environmental Protection Agency, Washington, D.C.

US EPA. 2011. 2012 National lakes assessment. Field Operations Manual. Office of Water, US Environmental Protection Agency, Washington, D.C.

US EPA. 2012. 2012 National lakes assessment site evaluation guidelines. Office of Water, US Environmental Protection Agency, Washington, D.C.

Wetzel, R.G. 2001. Limnology. 3rd ed. Lake and river ecosystems. Academic Press, San Diego, Calif.

Yuan, L.L., and Pollard, A.I. 2017. Using national-scale data to develop nutrient–microcystin relationships that guide management decisions. Environ. Sci. Technol. **51**(12): 6972–6980. doi:10.1021/acs.est.7b01410. PMID:28561562.

Yuan, L.L., and Pollard, A.I. 2019. Combining national and state data improves predictions of microcystin concentration. Harmful Algae, **84**: 75–83. doi:10.1016/j.hal.2019.02.009. PMID:31128815.